Rheol Acta (2017) 56:801–810
DOI 10.1007/s00397-017-1040-1

ORIGINAL CONTRIBUTION

Dual yielding in capillary suspensions

Amit Ahuja[1] · **Chaiwut Gamonpilas**[2]

Received: 5 May 2017 / Revised: 12 July 2017 / Accepted: 14 August 2017 / Published online: 4 September 2017

Abstract Rheological measurements were performed to examine the yielding behavior of capillary suspensions prepared by mixing cocoa powder as dispersed phase, vegetable oil as the continuous primary fluid, and water as the secondary fluid. Here, we investigated the yielding behavior of solid-fluid-fluid systems with varying particle volume fraction, ϕ, spanning the regime from a low volume fraction ($\phi = 0.25$) to a highly filled regime ($\phi = 0.65$) using dynamic oscillatory measurements. While for $\phi \leq 0.4$ with a fixed water volume fraction (ϕ_w) of 0.06 as the secondary fluid, capillary suspensions exhibited a single yield point due to rupturing of aqueous capillary bridges between the particles, while capillary suspensions with $\phi \geq 0.45$ showed a two-step yielding behavior. On plotting elastic stress ($G'\gamma$) as a function of applied strain (γ), two distinct peaks, indicating two yield stresses, were observed. Both the yield stresses and storage modulus at low strains were found to increase with ϕ following a power law dependence. With increasing ϕ_w (0 – 0.08) at a fixed $\phi = 0.65$, the system shifted to a frustrated, jammed state with particles strongly held together shown by rapidly increasing first and second yield stresses. In particular, the first yield stress was found to increase with ϕ_w following a power law dependence, while the second yield stress was found to increase exponentially with ϕ_w. Transient steady shear tests were also performed. The single stress overshoot for $\phi \leq 0.4$ with $\phi_w = 0.06$ reflected one-step yielding behavior. In contrast, for high ϕ (≥ 0.45) values with $\phi_w = 0.06$, two stress overshoots were observed in agreement with the two-step yielding behavior shown in the dynamic oscillatory measurements. Experiments on the effect of resting time on microstructure recovery demonstrated that aggregates could reform after resting under quiescent conditions.

Keywords Capillary suspensions · Yield stress · Rheology · Elastic stress · Structure-property

✉ Amit Ahuja
amitahuja502@gmail.com

Chaiwut Gamonpilas
chaiwutg@mtec.or.th

[1] Benjamin Levich Institute and Department of Chemical Engineering, City College of City University of New York, 160 Convent Avenue, New York, NY 10031, USA

[2] Polymer Physics Laboratory, National Metal and Materials Technology Center, 114 Thailand Science Park, Pahonyothin Road, Khlong Luang, Patumthani 12120, Thailand

Introduction

The processes such as mixing, pumping, filling, and packaging involved in the production of many food products are associated to the complex flow of materials. Processing of viscoelastic materials with high viscosity and yield stress is a challenging industrial issue. Examining the impact of microstructure on the rheological behavior is pivotal for stability of products, quality control, consumer perceived properties and also to economically process the products at manufacturing plants. Recently, the role and usefulness of capillary interactions in tuning the complex flow behavior of solid particle suspensions have received significant attention in the literature (Koos and Willenbacher 2011; Koos et al. 2014; Koos 2014; Bossler and Koos 2016).

Using the capillary forces, rheological properties, stability against sedimentation, and textural properties can be adjusted extensively to meet the needs of formulation and processing (Hoffmann et al. 2014; Wollgarten et al. 2016). Apart from their potential usage in the formulation and processing of consumer goods, capillary forces have also been shown to play an important role in the rheology of hydrate slurries in the oil industry (Zylyftari et al. 2013; Ahuja et al. 2014, 2015; Ahuja 2015; Zylyftari et al. 2015; Karanjkar et al. 2016). Mixing a small volume of an immiscible fluid to a particle suspension can induce particle agglomeration as a result of capillary bridging between the particles. This effect leads to a material transition from a simple suspension to a viscoelastic paste-like material and it has been shown to impact the resulting rheological behavior tremendously (Koos and Willenbacher 2011). Based on the contact angle of the secondary phase with the particles, two different states of bridges, namely pendular and capillary, can be obtained. If the secondary fluid preferentially wets the particles, a meniscus, formed between the particles, leads to a pendular state. On the other hand, if the secondary fluid does not wet the particles, clustered particles in the vicinity of a small volume of secondary fluid results in capillary state (Koos et al. 2014). The capillary force controls the state of bridges between the particles and can be used to tune the rheological behavior of capillary suspensions by modifying the volume of secondary phase, particle size, interfacial tension between the two fluids. The magnitude of the capillary force between the bridged particles is found to be inversely proportional to the particle radius and is directly proportional to the interfacial tension which can in turn be manipulated by temperature and by the use of surfactant (Koos et al. 2012).

Understanding the role of capillary bridges in tailoring the flow behavior of fluid-fluid-solid system is of great industrial significance. Hoffmann et al. (2014) and Wollgarten et al. (2016) studied two simple model systems, important to food industry, where capillary bridging has been shown as a new route for the formulation of next generation low-fat food products. Hoffmann et al. (2014) studied the stability and rheology of two food model systems, namely corn starch and cocoa particles, with vegetable oil as the primary fluid and water as the secondary fluid. The formation of capillary bridges between the cocoa particles were shown to improve the heat stability, texture, and rheological properties of the model chocolate system. Wollgarten et al. (2016) demonstrated that on heating a cocoa particle-based simple suspension up to a certain temperature, residual cocoa butter (fat) in semi-crystalline form releases as thin layers around particles. This subsequently leads to the formation of bridges between the particles shown by more than two orders of magnitude increase in viscosity and yield stress. Above a certain temperature, the cocoa butter separates out in the continuous phase as a result of which the networked structure collapses.

Here, we extend the works of Hoffmann et al. (2014) and Wollgarten et al. (2016) on cocoa capillary suspensions by investigating the role of composition of ternary admixture on the rheological behavior over a wide range of composition. Specifically, we focus our attention to the yielding mechanism of solid-fluid-fluid systems with varying ϕ spanning the regime from a low volume fraction ($\phi = 0.25$) to a highly filled regime ($\phi = 0.65$). We observed an interesting two-step yielding process in the cocoa particle-based capillary suspensions. We probed this behavior in detail and proposed plausible mechanisms for the observed two-step yielding behavior. Previous rheological studies on capillary suspensions have primarily focused on the measurements of increased rheological response by increasing wetting fluid loadings, particle size, and interfacial manipulations and have been limited to low to moderate particle volume fractions ($\phi \leq 0.4$). Though this two-step yielding mechanism has been observed in a wide variety of different systems. For example, Koumakis and Petekidis (2011) used chemically grafted PMMA particle dispersed in *cis*-decalin and investigated the yielding behavior of attractive glassy phase at high particle concentrations and attractive gel phase at lower particle concentrations while keeping the attraction strength constant. They noted a two-step yielding behavior for both the systems. The first yielding step was ascribed to the event of bond breaking while the second step was associated to the breaking of particle agglomerates into smaller fragments. Recently, Zhou et al. (2014) investigated the yielding behavior of a core-shell microgel system synthesized by an emulsion polymerization reaction using polystyrene as core and poly(*N*-isopropylacrylamide) as shell. By varying the shell/core ratio in the synthesis, microgels of different shell thickness were obtained. Different yielding behaviors were observed; at low and high ratios, one-step yielding was observed while for an intermediate ratio, a two-step yielding behavior occurred. The first yielding event was attributed to the deformation of soft shell, while the second to the collision of the hard cores.

Shao et al. (2013) carried out the rheology of aqueous carbopol microgel in which transition from a repulsive glass to an attractive gel was achieved with the addition of salt. It was concluded that the system exhibited a single-step yielding when the interactions are repulsive and a two-step yielding when interactions are primarily attractive. The two peaks observed in loss modulus were associated to network rupture and cluster breakup. Shukla et al. (2015) noted two-step yielding in surfactant pastes containing abrasive and clay particles, typically used in commercial dishwash

liquids. The origin of first yielding was attributed to the rupture of network structure formed by the particles and the second yielding was due to the breaking of particle agglomerates. Segovia-Gutiérrez et al. (2012) reported two-step yielding in a magneto-rheological model fluid of carbonyl iron particles dispersed in silicone oil. With lower particle loadings, only one-step yielding was detected while higher iron particle loadings led to two-step yielding. Above a critical particle concentration, fractal flocs of particles come closer and subsequently form networks. These cluster-cluster bonds break at higher stress amplitudes causing the second yielding step. Datta et al. (2011) studied attractive emulsions and reported the occurrence of two-step yielding above random close packing concentrations. Sentjabrskaja et al. (2013) performed rheological measurements on binary colloidal glasses and reported two-step yielding attributing the two steps to two existing characteristic length scales corresponding to caging of small and large particulates of the binary system. Chan and Mohraz (2012) investigated two-step yielding process in a dilute colloidal gel obtained by sterically stabilized PMMA particles in a mixture of *cis*-decahydronaphthalene and cyclohexyl bromide. Interestingly, they showed that the first yielding in dilute colloidal gels is due to bond rotation and the second yield point is due to bond rupture unlike dense systems where bond rupturing is the prime reason for the first yielding and cage breaking leads to the second yielding.

Clearly, the commonality among all the different systems, discussed above, exhibiting two-step yielding behavior is the existence of two interaction forces at the particulate level or two competing characteristic length or time scales. This paper aims to provide a new insight on the yielding behavior of capillary suspensions. Particularly, we report the combined impact of capillary bridging and networked particulate structures, studied by varying water fraction and particle loadings, respectively, on the yielding behavior of the suspensions. We present results obtained from oscillatory strain sweeps and transient steady shear experiments and demonstrate two-step yielding, previously unreported, for capillary suspensions. Though Domenech and Velankar (2015) briefly mentioned the appearance of a second shoulder for both storage and loss moduli at larger strain in their ternary system of capillary suspension consisting of polyisobutylene as a continuous phase, polyethylene oxide as the secondary phase and silica particles as a dispersed phase.

Materials and methods

Cocoa powder (Hershey Company) was purchased from the local supermarket to prepare cocoa suspensions. The cocoa particles were unsweetened and non-alkalized and had a fat content of 1%. These particles were used as provided without further purification or chemical treatment. The particle size was measured using a laser diffraction particle size distribution analyzer (Horiba, LA-300). The particles were dispersed in distilled water and sonicated before particle size measurement. The particle size distribution is shown in Fig. 1. Cocoa particles have Sauter mean diameter of $d_{3,2} = 16.1\ \mu$m. Food grade vegetable oil (100% soybean, Stop & Shop brand) with a viscosity of 45 mPa.s at 25 °C and a density of 0.88 g/cm^3 was purchased from a local supermarket. Deionized water was used from a Millipore QTM system. Cocoa particles were mixed into the oil using a mechanical mixer (IKA, Eurostar 60) at 500 rpm until a homogenous mixture is obtained. A known amount of water was subsequently mixed to the suspension at 1000 rpm for 5 min. The mixing speed and time were kept fixed to prepare samples in this study, and this protocol allowed us to do measurements with a good reproducibility (see Fig. S1). Though, mixing conditions play an important role and has been shown to influence the rheological properties of the prepared capillary suspensions tremendously by Bossler et al. (2017) recently. In order to investigate the impact of mixing on the rheological properties of cocoa suspensions, we performed some additional experiments and results are discussed in the supplementary information (see Fig. S2a-b). Rheological measurements were carried out using a rotational rheometer (ARES G2, TA Instruments) equipped with a cylindrical cup and a four-blade vane rotor. The cup has a diameter of 30 mm and vane rotor diameter is 15 mm. A vane-in-cup geometry is used to prevent wall slippage. Sample was loaded carefully in the cylindrical cup from the air-tight containers. All measurements were performed at a fixed temperature of 25 °C. Microscopic images were taken using Olympus BX-51 and GelSight microscopes.

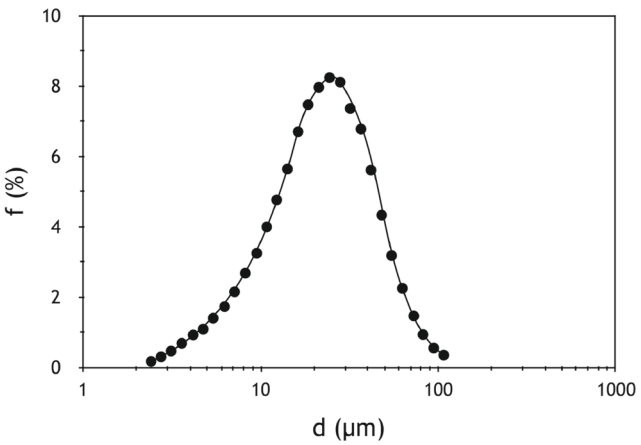

Fig. 1 Particle size distribution of cocoa particles dispersed in distilled water

Results

Figure 2 shows storage modulus (G′) plotted as a function of amplitude of oscillatory strain (γ) at a frequency (f) of 1 Hz for different cocoa particle volume fractions (ϕ) covering a low ϕ (= 0.25) to a highly filled regime at high ϕ (= 0.65) with a fixed $\phi_w = 0.06$ (based on total volume), where ϕ_w is the volume fraction of secondary phase (water). Clearly, at lower strain limits, G′ remains constant showing a linear viscoelastic regime for all values of ϕ. Above a critical strain, sample begins to yield as indicated by a decrease in G′. For higher ϕ ($\geq$ 0.5), G′ continues to decrease and exhibits a small to wide (depending on the value of ϕ) second plateau. When a second critical strain is attained, G′ decreases further and the whole curve clearly shows two distinct yield points indicating yielding through two mechanisms. As ϕ is reduced, the second shoulder in G′ becomes less prominent towards the higher magnitudes of strain and completely disappears for $\phi \leq 0.4$. The behavior of G″ along with G′ is shown only for $\phi = 0.65$ in the inset for clarification purposes.

In Fig. 3a, we show the elastic stress, G′γ, as a function of applied γ for varying ϕ by simply recasting the data from Fig. 2. In this plot, the two yield points can be seen more clearly indicating two yielding mechanisms in action, where the elastic stress shows two peaks for all $\phi \geq 0.45$. For smaller values of ϕ ($\leq$ 0.4), there was no second peak suggesting only one-step yielding. To clearly demonstrate this transition from one-step to two-step yielding in going from $\phi = 0.4$ to 0.45, an inset plot with relevant axis scale is shown in Fig. 3a. A broad maximum is observed for $\phi \leq$ 0.4, which suggests a gradual yielding of the material presumably due to elongation and stretching of bridges in the agglomerates. Furthermore, in Fig. 3b, we plot G′ as a function of magnitude of measured oscillatory stress (σ) for f = 1 Hz. The second yielding step is distinctly seen by a smaller plateau-like portion of the curve of G′ versus σ. However, this region becomes progressively less pronounced with the decrease in ϕ and completely disappears for $\phi \leq 0.4$. Plotting the data shown in Fig. 2 in these two different ways in Fig. 3a, b allows us to view the plateaus before yielding more explicitly and further confirms the existence of two yield points. Figure 4a, b show microscopic images of the cocoa suspension in oil for $\phi = 0.25$ and 0.45 and a fixed $\phi_w = 0.06$, respectively. As can be seen in these micrographs that for $\phi = 0.25$, the large cocoa agglomerates are either present as discrete structures or weakly connected to each other, while on the other hand for $\phi = 0.45$, there is a continuous, sample-spanning, tightly-packed networked structure of agglomerates. These images show very compact structures along with strand-like (likely pendular) aggregates in the samples. These large structures are capillary aggregates, where particles form a raspberry-like structure with the secondary fluid phase. Some additional microscopy experiments performed at lower particle volume fractions indicate that these clusters are connected via menisci (see Fig. S3). There are several possible mechanistic pictures one can draw to explain the microstructural origins of these distinct yielding transitions. At this stage, it is difficult to present an exact mechanistic picture and it warrants further studies to examine the microstructural origins of these distinct yielding transitions. The first possibility is that for cocoa suspensions with low volume fraction of particles ($\phi < 0.4$), there is not a strong global network structure between the cocoa particle agglomerates. On applying a strain smaller than the first yield strain, the capillary bridges between the particles inside agglomerates will elongate and outstretch though the agglomerates remain intact. With increasing amplitude of oscillatory strain (greater than yield strain), the capillary bridges begin to break apart and agglomerates are broken which imparts fluidity to the system. In concentrated suspensions ($\phi \geq 0.45$), apart from locally formed capillary bridges within agglomerates, the interconnectivity of several agglomerates also becomes more pronounced as seen in Fig. 4b. The networked structure fragments at the first yield strain, which results in large agglomerates in a fluidized state in which individual particles remain in the jammed or locked state due to liquid capillary bridges between the particles. When the amplitude of applied oscillatory strain exceeds the second yield strain, the capillary bridges rupture and the clusters break into smaller fragments, thus leading to complete yielding of the material. Some additional images (Fig. S4a–c) taken using GelSight microscope are provided in the supplementary information. The second explanation could be due to a sequence of bond rotation with structural rearrangements, followed by bond breakage and network

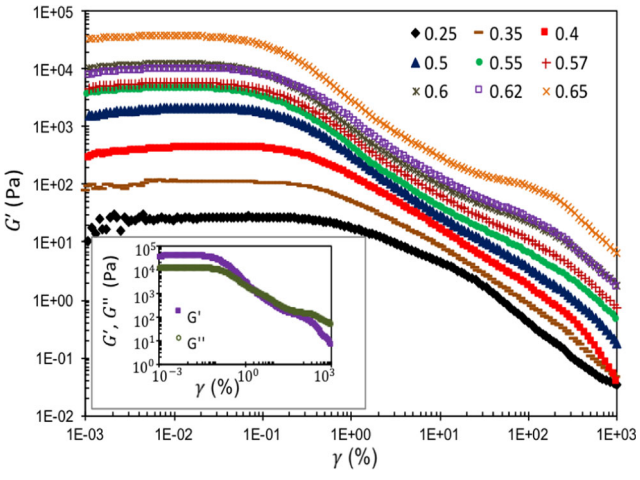

Fig. 2 Behavior of G′ is plotted as a function of γ in a dynamic strain sweep experiment carried out at f = 1 Hz on cocoa suspensions with varying ϕ (shown in legend) and with a fixed $\phi_w = 0.06$. The inset shows the behavior of both G′ and G″ for $\phi = 0.65$

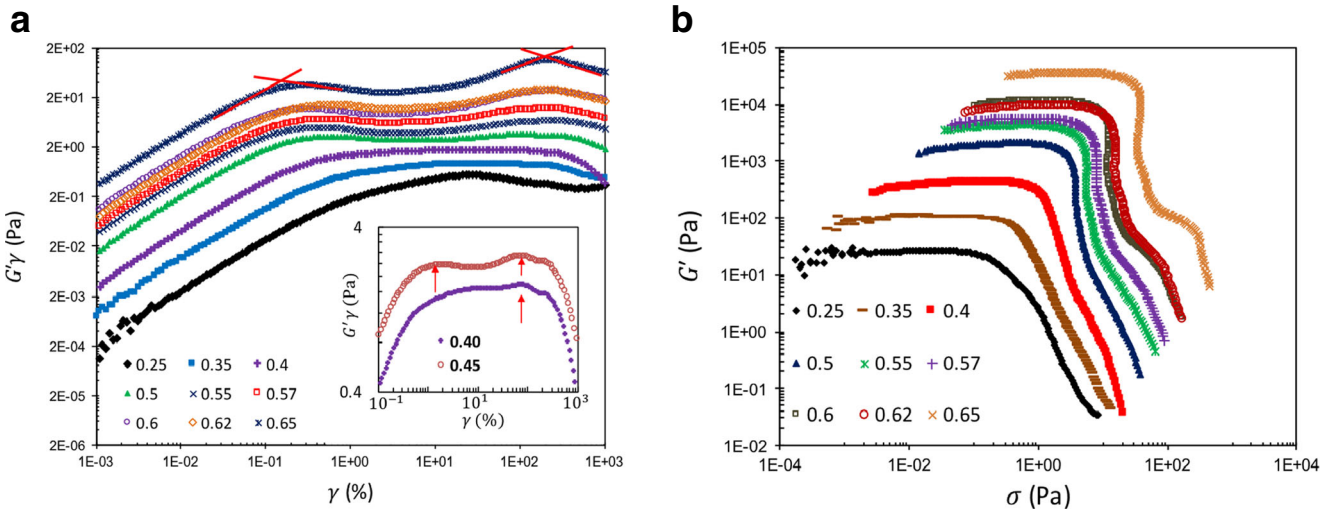

Fig. 3 **a** Elastic stress, G′γ, as a function of γ for varying ϕ (shown in legend). The red intersecting lines indicate two yield points and the onset of nonlinear behavior. The inset shows the behavior of suspension with $\phi = 0.4$ and 0.45 with expanded axis scale, indicating only one-step and two-step yielding (shown by vertical red arrows). **b** G′ versus measured σ for varying ϕ (as shown in legend) with equal content of aqueous secondary phase. Both (**a**) and (**b**) are the same data as shown in Fig. 2

failure as proposed by Chan and Mohraz (2012). The third plausible hypothesis is the distribution and polydispersity in droplet sizes, which could form liquid bridges of varying sizes between the particles and agglomerates where smaller bridges possibly rupture at smaller strains resulting in first yielding before complete yielding of the suspensions at higher amplitudes of strains. Another possible scenario that could explain the observed transition from a single to two-step yielding may be a transition from a capillary dominated system at high relative secondary fluid volume fraction to a system at low relative fluid contents. To address this point, we performed additional experiments with $\phi = 0.4$ and 0.5 and water volume-to-particle volume fraction ratio (ρ) ranging from 0.005 to 0.25 (for ϕ_w varying from 0.002 to 0.125) and the results are shown in Fig. S5 in the supplementary information. For both values of ϕ, there was no measureable yield stress for $0.005 \leq \rho < 0.04$. For $\phi = 0.4$, there was only one yield point for $0.04 \leq \rho \leq 0.25$. While for $\phi = 0.5$, we noted two yield points in the entire range $0.04 \leq \rho \leq 0.25$ ($\phi_w = 0.02 - 0.125$). This demonstrates that the observed transition from single- to two-step yielding is not due to a transition from a capillary-dominated water-rich system to a water-deficient system.

The presence of two plateaus or shoulders in a typical plot of measured G′ with applied γ in a dynamic oscillatory experiment is a classic hallmark of the presence of wall slippage in the system. Walls et al. (2003) studied the yielding behavior of colloidal gels containing hydrophobic silica, polyether, and lithium salts. They observed two plateaus in storage modulus (or two maxima in elastic stress), which were attributed to wall slippage (due to particle-lean thin layer in the vicinity of walls) and yielding of the colloidal gel. A plausible mechanistic explanation of the observed two plateaus in our system on plotting G′ with γ could also be due to the presence of dominant slippage at the walls and yielding of the material. In order to investigate the

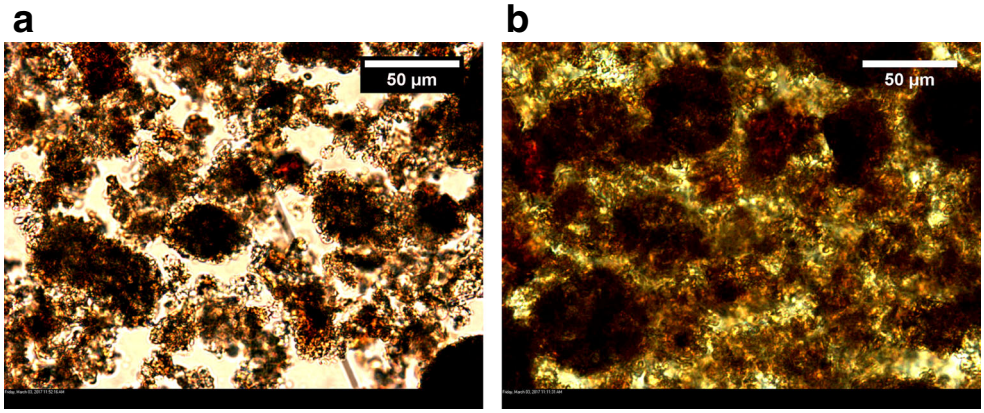

Fig. 4 Microscopic images of capillary suspensions made from cocoa powder in oil with a fixed $\phi_w = 0.06$ (**a**) $\phi = 0.25$, (**b**) $\phi = 0.45$

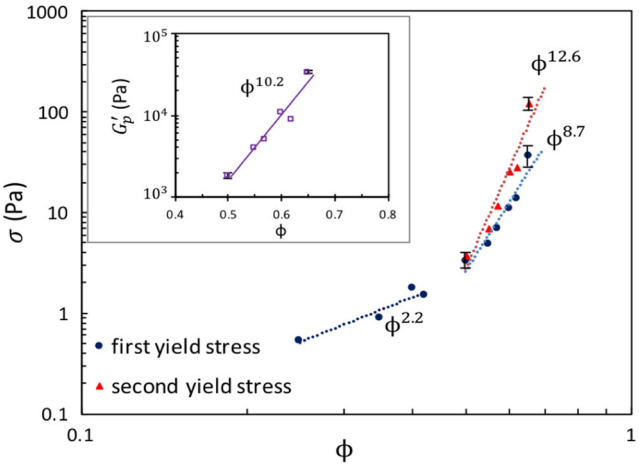

Fig. 5 The first and second yield stresses plotted as a function of ϕ. The inset shows the average values of storage modulus plateau at low strains with ϕ. The lines are power law fits to the data

origin of the observed two plateaus in our system, we performed additional experiments using different geometries and results are shown in the Fig. S6 in the supplementary information. To this end, we used a serrated cup with a vane rotor on a stress-controlled rheometer (AR 2000ex, TA Instruments). The serrated cup (roughness $\sim$ 500 μm) has a diameter of 30 mm and vane rotor diameter is 15 mm. The results are compared in the Fig. S6(a) for $\phi = 0.6$ and 0.65 with $\phi_w = 0.06$ obtained using a smooth cup (using ARES-G2 rheometer) and a serrated cup along with a vane rotor. A good match between these measurements clearly indicates the absence of slippage at the cup wall. Additionally, we used serrated parallel plates (40-mm diameter, AR 2000ex) at different gaps for a suspension with $\phi = 0.65$ and $\phi_w = 0.06$ (Fig. S6b). Both the plates are serrated. The presence of two-step yielding can be seen very clearly with serrated geometries, which suggests that the two yield points are indeed due to two microstructures present in the system rather than any artifact or anomaly due to slippage.

The yield stresses corresponding to first and second yield steps from maxima in elastic stress (Fig. 3a) along with low strain storage modulus plateau (G_p') values as a function of ϕ are plotted in Fig. 5. Both the yield stresses and G_p' values were found to increase with ϕ following a power law dependence with exponents of 8.7, 12.6 and 10.2, respectively, for $\phi \geq 0.5$. The value of power law exponent is indicative of the degree of connectivity and packing of the networked microstructure. Thus, a high value of exponent, as noted here, is representative of a compact structure. As discussed earlier in Fig. 3a, the yield stress can be considered as the product of G_p' and the yield strain ($\sigma = G_p'\gamma$). As a result of this, the yield stresses increase rapidly with increasing ϕ primarily due to the strong dependence of G_p' on ϕ. This type of strong dependence of yield stresses and G_p' on ϕ (higher exponents) has been observed in a variety of other systems as well (Zhao et al. 2014; Zhou et al. 2014; Domenech and Velankar 2015). For $\phi < 0.5$, the first yield stress also increases with a power law dependence on ϕ but with a much smaller exponent of 2.2.

Figure 6 shows behavior of G′ as a function of increasing γ for $\phi = 0.65$, $\phi_w = 0.06$ and f = 0.05, 0.1, and 1 Hz. It can be observed that the dependence of G′ on γ shows distinct variation with change in frequency. G′ and G″ follow linear viscoelastic behavior in the limit of small strains. The material yields subsequently with increase in the amplitude of strain. With increasing frequencies, the two-step yielding behavior with a small increase in G_p' values and a shift of second yield point towards higher strains was observed while no significant effects were found on the first yielding

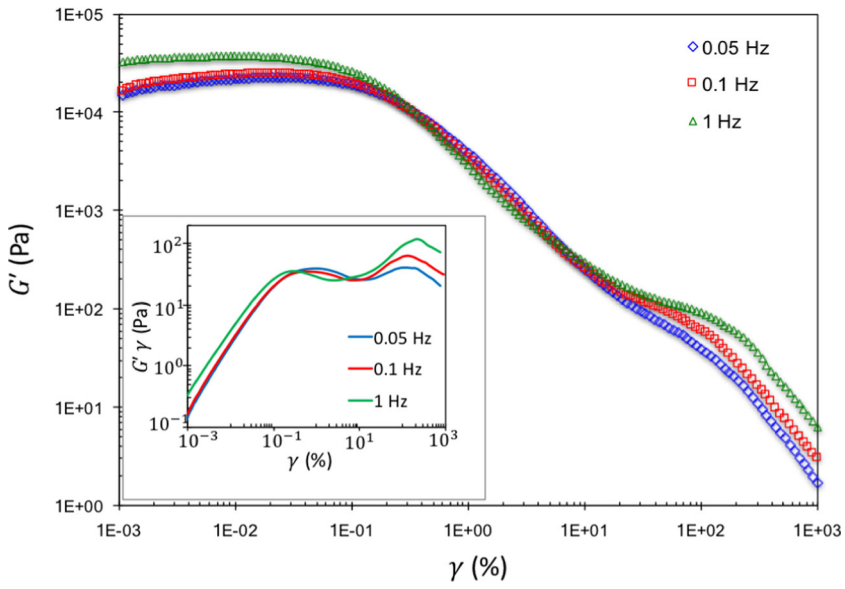

Fig. 6 Dynamic strain sweep of cocoa suspension with $\phi = 0.65$ and $\phi_w = 0.06$ at different frequencies

event with increasing frequencies. The inset shows the effects of frequencies on the first and second maxima in elastic stress.

Figure 7a shows dynamic strain sweep at f = 1 Hz on cocoa suspensions with a fixed $\phi = 0.65$ and with varying ϕ_w in the range of 0.02 – 0.08. On increasing ϕ_w from 0 to 0.08, G'_p increases dramatically from $O(10^2)$ to $O(10^5)$. Figure 7b-d show yield stresses (σ_1, σ_2) obtained from maxima in elastic stress along with G'_p with varying ϕ_w. While σ_1 and G'_p are found to increase with ϕ_w following a power law dependence, σ_2 followed an exponential law dependence on ϕ_w as shown in Fig. 7b-d. This further confirms the formation of a networked structure which breaks down via two-step yielding mechanism. The increase in both yield stresses with increasing ϕ_w indicates increased interconnectivity, stronger networked structure and larger clusters with increased heterogeneity in the sample, that require higher stresses to break down. Similar experiments with lower values of $\phi = 0.55$ and $\phi = 0.5$ and varying ϕ_w (0 to 0.07) were conducted. As can be seen, even at lower values of ϕ, there is a power law dependence of the first yield stress on ϕ_w, while an exponential law dependence of the second yield stress on ϕ_w was still valid.

As pointed out by Koumakis and Petekidis (2011), step shear tests are comparatively simpler and quicker than oscillatory experiments to study the nonlinear response of complex systems. To investigate the nonlinear response of the cocoa suspensions, steady shear tests were carried out, in which samples were subjected to a fixed shear rate for a fixed duration and the stress response was recorded. In

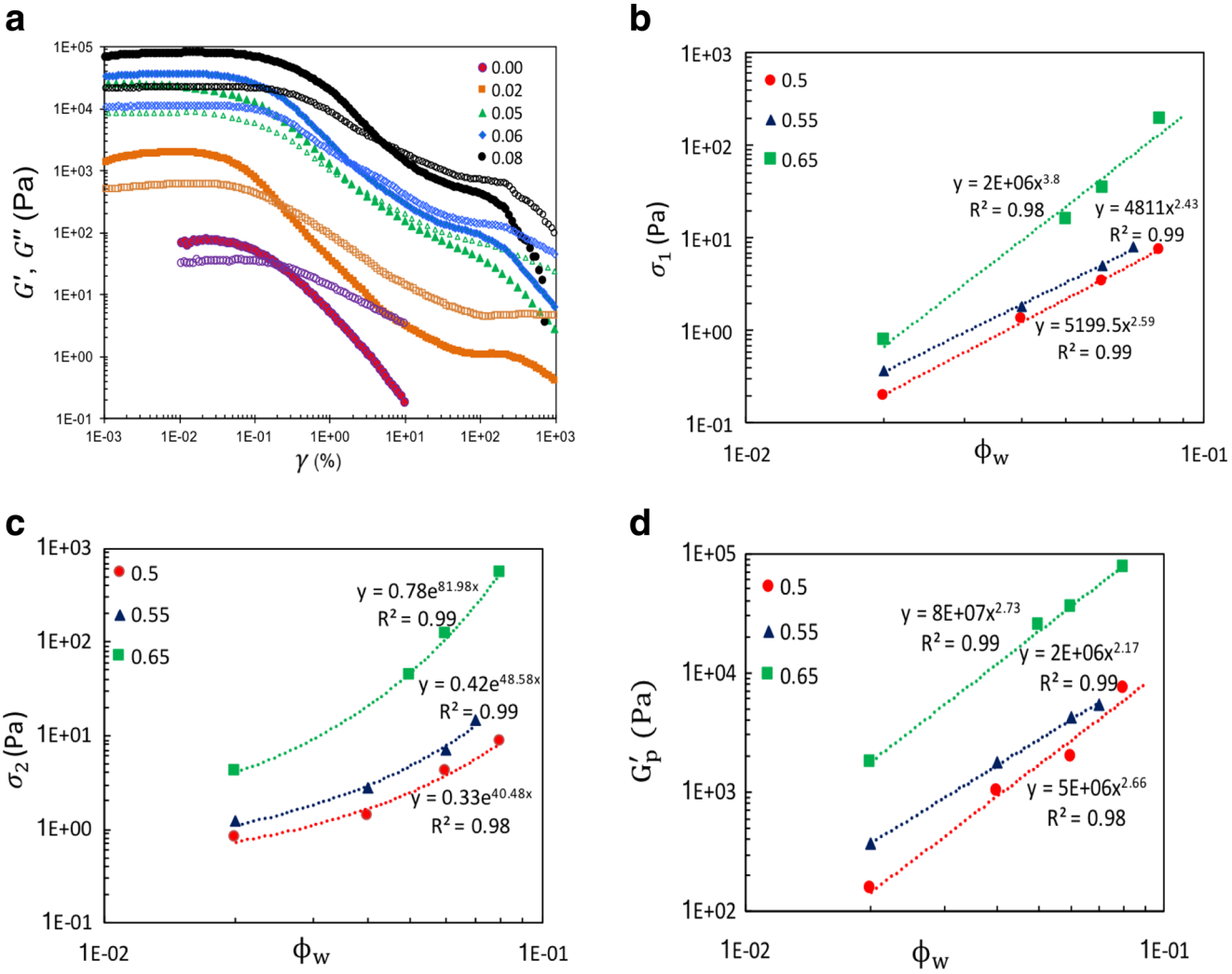

Fig. 7 **a** Behavior of G′ and G″ plotted as a function of magnitude of oscillatory strain in a dynamic strain sweep experiment carried out at f = 1 Hz on cocoa suspensions with a fixed $\phi = 0.65$ and with varying ϕ_w based on total volume (shown in legend). The total solid volume fraction was kept fixed while the volume of oil was adjusted to account for the varying water volume fraction. (G′: solid symbols, G″: open symbols). **b**, **c**, **d** The first and second yield stresses obtained from maxima in elastic stress and G'_p plotted as a function of ϕ_w for three different values of ϕ (shown in legend)

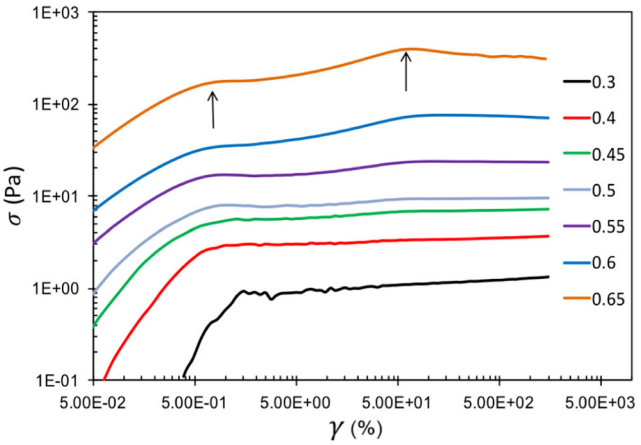

Fig. 8 Step rate tests showing stress response as a function of % strain at a rate of 0.5 s^{-1} for suspensions at various ϕ and $\phi_w = 0.06$

order to further corroborate our findings, we performed step rate tests on samples with various ϕ and at a fixed $\phi_w = 0.06$ and the results are shown in Fig. 8. At smaller γ ($< 2\%$), σ increases linearly indicating an elastic response. This is due to the presence of the capillary bridges between the particles. Beyond the first stress overshoot, for $\phi \leq 0.4$, the curves attain a plateau, exhibiting a single-step yielding. The single stress overshoot for $\phi \leq 0.4$ reflected the one-step yielding mechanism corresponding to rupturing of capillary bridges in agglomerates. In contrast, for high values of ϕ (≥ 0.45), two stress overshoots were observed in agreement with the two-step yielding behavior shown in the dynamic oscillatory measurements. Also as ϕ increases, both the yield stresses increase as noted earlier in the dynamic oscillatory measurements. Other experiments were carried out to investigate the effects of rest time on the recovery of microstructure and the overall bulk rheological properties. Figure 9 shows the effect of rest time on the recovery of suspensions prepared at $\phi = 0.45$, 0.60, and 0.65 and a fixed $\phi_w = 0.06$ after undergoing a full strain sweep from 0.001 to 1000% at a frequency of 1 Hz. The rest time is defined as the time given to the suspension under no shearing, measured from the cessation of dynamic oscillations in the experiments performed here. Interestingly, little or no quantitative changes in both the yield stresses, measured after a rest period of 2 h, were observed, which suggest that the original microstructure recovers almost completely within 2 h after the first strain sweep. The inset shows G′ plotted as a function of oscillatory strain for $\phi = 0.65$ and $\phi_w = 0.06$ after 40 min of rest time, demonstrating only partial recovery of the structure.

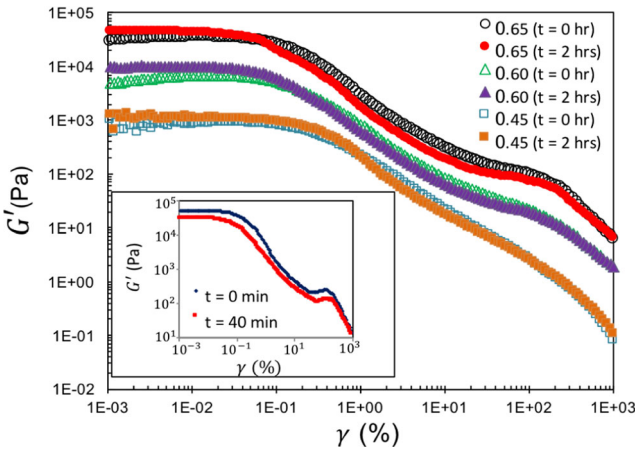

Fig. 9 Behavior of G′ is plotted as a function of magnitude of oscillatory strain in a dynamic strain sweep experiment carried out at a frequency of f = 1 Hz for freshly prepared suspensions (open symbols) at various ϕ (in legend) and $\phi_w = 0.06$. Solid symbols represent G′ data measured after a rest time of approximately 2 h on the same suspensions. The inset shows G′ plotted as a function of oscillatory strain for $\phi = 0.65$ and $\phi_w = 0.06$ after 40 min of rest time showing partial recovery of the structure

Discussion

A systematic design of experiments with a suspension system of cocoa particles dispersed in oil with small amount of water as secondary fluid was conducted to probe the yielding behavior of capillary suspensions in detail. Interestingly, these capillary suspensions exhibit dual yielding behavior. Figure 2 shows strain amplitude sweep response of cocoa suspension at f = 1 Hz for various values of ϕ. At small γ, G′ is greater than G″ showing that the samples are solid-like, and G′ and G″ are constant in this regime which indicates the linear viscoelastic response. In all cases, G′ decreases at higher γ until it eventually becomes smaller than G″ suggesting that the samples have yielded to become flowable. The samples show a single yielding for $\phi < 0.4$ and exhibit two shoulders for $\phi \geq 0.45$. The two shoulders of G′, a clear signature of dual yielding, become more pronounced with increasing ϕ.

The first yield strain is associated to the spacing between agglomerates when shearing leads neighboring agglomerates to collide. As ϕ decreases at a fixed ϕ_w (Figs. 2 and 3a), the first yield strain values increase indicating that at lower particle concentrations there is a higher flexibility (at cluster-cluster level) which permits significant degree of freedom and elongation before network fracture. This is in agreement with the works of Koumakis and Petekidis (2011) and Shukla et al. (2015). Shukla et al. (2015) showed that in surfactant pastes, for 30 and 45 wt.% abrasive particles the strain at the first yield event is smaller in comparison to no particle case. Though the corresponding stresses with higher particle loadings were higher, attributed to higher values of storage modulus associated with the gels having higher particle concentrations. Similarly, Koumakis and Petekidis (2011) found that the values of strains corresponding to

first yield point spanned in two regimes of particle volume fractions; the yield strain is lower for $\phi > 0.4$ and is approximately constant. On the other hand, as ϕ_w increases for a fixed ϕ, the first yield strain is found to be increasing significantly as can be seen in Fig. 7a. As the volume of added water increases for the same particle loadings, the degree of percolation increases due to an increase in the number density of cluster-cluster connections and an increase in the volume of meniscus at every cluster-cluster connection which presumably require higher strains to break.

Regarding the second yield strains, there are opposing trends reported in the literature, which appear to be system dependent (Shukla et al. 2015; Koumakis and Petekidis 2011; Shao et al. 2013). Shukla et al. (2015) reported an increase in the values of second yield strain with an increase in particle loadings in suspension pastes and Shao et al. (2013) also observed an increase in the second yield strain with an increase in attraction force in carbopol gels. While Koumakis and Petekidis (2011) noted a decrease in the second yield strain with increasing PMMA particle fractions in their system. In our system, for a fixed ϕ and decreasing ϕ_w, the second yield strain was observed to be increasing, presumably due to a reduced degree of agglomeration at lower ϕ_w. This could possibly enhance the voidage in the system rendering it more heterogeneous. As a result of this, the fluidized clusters (after the first yield point) attain a higher degree of movement and rotation with shearing and thus a higher second yield strain is observed. The observed trends for the first and second yield strains are shown explicitly as elastic stress versus γ for $\phi = 0.55$ and varying ϕ_w in Fig. S7. Figure 6 illustrates the effects of increasing frequency on the dual yielding behavior of the capillary suspensions by performing strain sweeps. On increasing the frequency from 0.05 to 1 Hz, the first yield strain (corresponding to elastic stress maxima) was found to decrease from 1 to 0.3%. The first yield stress was also found to decrease slightly from 38.2 to 35.2 Pa for the same frequency increase. As can be seen in Fig. 6, G'_p increases slightly with increasing frequency. The net effect of increased G'_p and decreased first strain is to give a somewhat lower first yield stress. Although, this cannot be considered a strong dependence of the first yielding event on frequency as the observed quantitative differences are within the experimental uncertainty. Interestingly, the second yield strain and stress were found to be increasing prominently with increasing frequency. For a frequency increase of 0.05 to 1 Hz, the second yield strain increased from 131.5 to 208%, while the second yield stress increased by approximately 3 times from 39.6 to 117.7 Pa. The dependence of the first and second yielding events on frequency appear to be system specific; there are conflicting observations in the literature. Shukla et al. (2015) noted that the first yield strain and stress are independent of frequency for the suspension pastes. While the second yielding event was found to occur at lower strains. Shao et al. (2013) showed a stronger dependence of loss modulus on frequency while there was a weak or no dependence of low strain storage modulus and yield strains on frequency. Koumakis and Petekidis (2011) found the first yielding strain to be independent of frequency for the PMMA particles at volume fractions of 0.4 to 0.6, while the strain associated to second yielding event was reported to be decreasing with the increasing frequencies. The exact mechanism behind the observed trends regarding the dependence of frequency on second yielding event in our system is unclear and requires further detailed examination. It should be noted that an increase in the frequency of oscillations decreases the deformation timescale. In an oscillatory experiment, the product of strain amplitude (γ) and frequency (f) can be considered as a magnitude of deformation rate. Thus, an amplitude sweep at a fixed frequency exposes samples to increasing strains as well as increasing deformation rates. It can be seen clearly that the stress and the strain at the first yielding point is not dependent on frequency. This suggests that the first yielding does not really depend on the timescale of deformation. The subsequent shearing of the fluidized aggregates is anticipated to generate significant stresses. Additionally, the roughness, irregular shape of the aggregate surface, and higher number density of these structures as well as the hydrodynamic lubrication may not prevent the physical contact between these particles/aggregates. The friction resulting from physical contacts would certainly add to overall stresses significantly (Shukla et al. 2015). The amplitude of these stresses is believed to be increasing with decreasing timescale of deformation field. This results into higher value of G' with increasing frequency particularly at higher strains (close to second yield point). The yield stress is interpreted as maxima in elastic stress ($G'\gamma$); a higher G' would result into higher yield stress.

Regarding the effects of rest time on capillary suspensions, Koos et al. (2014) showed that both storage and loss moduli increase with time and this aging process follows a power law. Our results indicate that the network recovers almost completely if allowed to rest under no shearing. In terms of G'_p, 60% of recovery takes place in the first 40 min for this particular case of $\phi = 0.65$ and $\phi_w = 0.06$. The first and second yield stresses were also observed to be smaller after 40 min of rest time in comparison to the original structure though full recovery was achieved in 2 h of rest period. During the first strain sweep, the sample is submitted to a strong oscillatory deformation and the material is in a completely fluidized state. After the cessation of dynamic oscillations, due to enhanced mobility the material undergoes accelerated restructuring and reorganization, which leads to a rapid increase in both the moduli and the network evolves and recovers almost completely over the investigated time window. However, further detailed study through

microscopic observation of the microstructure of suspension is required to understand the mechanism behind this reformation. Our results are agreeable with the recent work of Yang and Velankar (2017) which investigated the yielding behavior and microstructural recovery of pendular network suspensions using a refractive index matched system of glass particles as dispersed phase, isoprene as the primary continuous phase and glycerol as the secondary wetting fluid. Their work also demonstrated clearly that aggregates were broken apart via meniscus at higher shear rates but they reformed promptly under small shearing motion.

Conclusion

We probed the yielding mechanism in capillary suspensions at a fixed volume fraction of secondary phase which undergo a transition from a simple one-step yielding behavior at low particle volume fractions ($\phi \leq 0.4$) to a two-step yielding behavior at higher particle fractions ($\phi \geq 0.45$) due to combined interplay of networked structure and capillary bridges between the particles. Both the yield stresses and G'_p values were found to increase with ϕ following a power law dependence for $\phi \geq 0.45$. With increasing ϕ from 0.45 to 0.65 for a fixed $\phi_w = 0.06$, the second plateau becomes more prominent. The first yield strains were found to be decreasing with increasing values of ϕ at a fixed ϕ_w, while as ϕ_w increases for a fixed ϕ, the first yield strains were observed to be increasing significantly. On the other hand, the second yield strain values were observed to be increasing for a fixed ϕ and decreasing ϕ_w. On increasing ϕ_w from 0 to 0.06 while keeping ϕ fixed, the first yield stress showed a power law dependence on ϕ_w while the second yield stress followed an exponential dependence with ϕ_w. The sample microstructure recovers almost completely when a sufficient rest time was allowed for the material under no shearing.

Acknowledgments The authors appreciate discussions with Megha Goyal regarding the selection of low-fat cocoa powder and vegetable oil. We are also thankful to Prof. Jeffrey Morris (CUNY) for numerous useful discussions.

References

Ahuja A, Zylyftari G, Morris JF (2014) Calorimetric and rheological studies on cyclopentane hydrate-forming water-in-kerosene emulsions. J Chem Eng Data 60:362

Ahuja A, Zylyftari G, Morris JF (2015) Yield stress measurements of cyclopentane hydrate slurry. J Non–Newtonian Fluid Mech 220:116

Ahuja A (2015) Hydrate forming emulsion: Rheology and morphology analysis for flow assurance. PhD Thesis, City University of New York, New York

Bossler F, Koos E (2016) Structure of particle networks in capillary suspensions with wetting and nonwetting fluids. Langmuir 32:1489

Bossler F, Weyrauch L, Schmidt R, Koos E (2017) Influence of mixing conditions on the rheological properties and structure of capillary suspensions. Colloids Surf A Physicochem Eng Asp 518:85–97

Chan HK, Mohraz A (2012) Two-step yielding and directional strain-induced strengthening in dilute colloidal gels. Phys Rev E 85:041403

Datta SS, Gerrard DD, Rhodes TS, Mason TG, Weitz DA (2011) Rheology of attractive emulsions. Phys Rev E 84:041404

Domenech T, Velankar SS (2015) On the rheology of pendular gels and morphological developments in paste-like ternary systems based on capillary attraction. Soft Matter 11:1500

Hoffmann S, Koos E, Willenbacher N (2014) Using capillary bridges to tune stability and flow behavior of food suspensions. Food Hydrocolloids 40:44

Karanjkar PU, Ahuja A, Zylyftari G, Lee JW, Morris JF (2016) Rheology of cyclopentane hydrate slurry in a model oil-continuous emulsion. Rheol Acta 55:235

Koos E, Willenbacher N (2011) Capillary forces in suspension rheology. Science 331:897

Koos E, Johannsmeier J, Schwebler L, Wiillenbacher N (2012) Tuning suspension rheology using capillary forces. Soft Matter 8:6620

Koos E, Kannowade W, Willenbacher N (2014) Restructuring and aging in a capillary suspension. Rheol Acta 53:947

Koos E (2014) Capillary suspensions: particle networks formed through the capillary force. Curr Opin Colloid Interface Sci 19:575

Koumakis N, Petekidis G (2011) Two step yielding in attractive colloids: transition from gels to attractive glasses. Soft Matter 7:2456

Segovia-Gutiérrez JP, Berli CLA, De Vicente J (2012) Nonlinear viscoelasticity and two-step yielding in magnetorheology: A colloidal gel approach to understand the effect of particle concentration. J Rheol 56:1429

Sentjabrskaja T, Babaliari E, Hendricks J, Laurati M, Petekidis G, Egelhaaf SU (2013) Yielding of binary colloidal glasses. Soft Matter 9:4524

Shao Z, Negi AS, Osuji CO (2013) Role of interparticle attraction in the yielding response of microgel suspensions. Soft Matter 9:5492

Shukla A, Arnipally S, Dagaonkar M, Joshi YM (2015) Two-step yielding in surfactant suspension pastes. Rheol Acta 54:353–364

Walls HJ, Caines SB, Sanchez AM, Khan SA (2003) Yield stress and wall slip phenomena in colloidal silica gels. J Rheol 47(4):847

Wollgarten S, Yuce C, Koos E, Willenbacher N (2016) Tailoring flow behavior and texture of water based cocoa suspensions. Food Hydrocolloids 52:167

Yang J, Velankar S (2017) Preparation and yielding behavior of pendular network suspensions. J Rheol 61:217

Zhao C, Yuan G, Han JCC (2014) Bridging and caging in mixed suspensions of microsphere and adsorptive microgel. Soft Matter 10:8905

Zhou Z, Hollingsworth JV, Hong S, Cheng H, Han CC (2014) Yielding behavior in colloidal glasses: comparison between hard cage and soft cage. Langmuir 30:5739

Zylyftari G, Lee JW, Morris JF (2013) Salt effects on thermodynamic and rheological properties of hydrate forming emulsions. Chem Eng Sci 95:148

Zylyftari G, Ahuja A, Morris JF (2015) Modeling oilfield emulsions: comparison of cyclopentane hydrate and ice. Energy Fuels 29:6286